Indian Journal of Pure & Applied Physics
Vol. 60, February 2022, pp. 171-181

Effect of Annealing and Ion Beam Irradiation on AC Electrical Properties for Gold Sputtered PM-355

S I Radwan[a], A M Rashad[a,b], H R Tantawy[c] & S Abdel Samad[d]

[a]Accelerators and Ion Sources Department, NRC, Egyptian Atomic Energy Authority, Egypt

[b]Central Laboratory of Elemental and Isotopic Analysis, NRC, Egyptian Atomic Energy Authority, Egypt

[c]Chemical Engineering Department, Military Technical College, Egypt

[d]Experimental Nuclear Physics Department, NRC, Egyptian Atomic Energy Authority, Egypt

Received 15 August 2019; accepted 19 January 2022

Deposition of different gold thickness on PM-355 cleaned by ethanol forming thin films using magnetron sputtering. Gold layer with thickness 300, 400, 500, 700, 1000, 1300, and 1500 nm were deposited to prepare Au / PM-355 thin films. Then, ac electrical properties response of thin films for a wide frequency range 20Hz - 5MHz were measured at room temperature. Meanwhile, the measurements of ac conductivity, dielectric constant, and dielectric loss factor were plotted at different frequencies to determine the optimum thickness. Hence, the comparison was done between optimum Au thickness thin films cleaned by two organic solvents and ethanol before annealing at different frequencies. Also, study the effect of annealing and ion beam that extracted radially from conical anode and disc cathode ion source on optimum Au thickness thin film electrical properties. It is found that the annealing increases both dielectric constant, dielectric loss, and ac conductivity of optimum Au thin film at different frequencies. Despite, the nitrogen ion beam effected on these thin films by decreasing the dielectric constant and ac conductivity for all thin films except the chloroform one. Finally, study the comparison between the annealing and followed by ion irradiation thin films. It is noticed the decrease in ac electrical conductivity and dielectric constant at different frequencies.

Keywords: Thin film, PM-355, Gold, Sputtering, AC conductivity, Annealing, Dielectric constant, Ion beam, Dielectric loss.

1 Introduction

Plasma interactions technology such as etching, film deposition and surface modification has many applications especially in industry and research[1-3]. For a long time, the formation of coatings and thin films have various studies in science and technology[4-6]. Actually, the thin film deposition can be divided into the two essential technologies that are the physical and chemical vapor depositions[7]. A widely deposition technique based on a plasma vapor deposition process utilized for the well formation of thin films used in electrical, optical, medical and engineering applications is the magnetron sputtering[8-12]. The positively charged plasma is accelerated by applying the electrical field between a cathode (target) and an anode (substrate). When the plasma hits the target, its atoms are ejected to precipitate on the substrate material. A lot of studies were carried on the thin films and coatings especially produced using the magnetron sputtering with magnets used to control the transport of ions having a vital role in science and technology[13-15].

Polymers – metal combination that produce the change in the polymer optical and electrical properties is suitable for the electrical and optical devices, biomedical science, sensor technology, corrosion resistance, and *etc*[16-20]. Gold is a noble metal that used for various applications as in electronics, bio-sensing, optics, photonics and electrochemical devices[21-24]. Due to have high electrical conductivity, optical reflectivity, chemical and physical properties[25-27]. The information of polymers dielectric parameters is very essential in fabricating any electronic device[28-30]. Moreover, it is a vital requirement to further decrease the dielectric constant of polymers for widening the integrated circuits applications[31]. Due to the low cost of polymers, high accessibility and simple in preparation so they have wide applications in optics, nuclear track detectors, fuel cells[32-34]. Moreover, the metal coated with polymer membranes in different fuel cells[35,36].

*Corresponding author: (E-mail: torabsamah@yahoo.com)

The main objective of this study focused on the ac electrical properties of Au deposited on PM-355 which will be on interesting study for being used in fuel cell membrane. Hence, the preparation of Au/PM-355 thin films were done using magnetron sputtering with different Au thickness to determine the good properties of Au thickness. Moreover, study the effect of nitrogen ion beam extracted radially from the conical anode and disc cathode ion source to show how its influence on thin films electrical properties. Also, here study the effect of annealing, in the range of operating temperature proton exchange membrane fuel cell, on the formed thin films especially on the ac electrical conductivity. In future, study the effect of protons presented in the fuel cell on these thin films after impregnated on Nafion solution to be a membrane.

2 Magnetron Sputtering

Sputtering applications in aerospace, automotive components, data storage, sensors, surface acoustic wave devices and solar panels[37-40]. There are many physical vapor deposition methods for producing coatings involving thermal evaporation techniques and ionic sputtering methods that include ion-beam sputtering and magnetron sputtering[41,42]. Magnetron sputtering systems are concentrated on the well deposition from metal to compound through the ejection of atoms from a target in vacuum and fly into the substrate causing re-sputtering[43-46]. The advantages are to be performed under lower temperature, friendly to the environment, control the sputtering conditions for fabricating the very high purity films[47,48].

Thin film thickness and sputtering power usually play important roles in controlling the film properties[49]. So, we studied the effect of Au thickness, nm, on ac thin films electrical properties. Hence, PM-355 samples were firstly cleaned by ethanol and deposited by different Au thickness forming thin films. AC electrical properties were measured to determine the optimum thickness that achieve the good characteristic of thin film. This optimum thin film is compared with the exposure by annealing and ion beam ones after deposition. Also, we put in a comparison with chloroform cleaning PM-355 sample before deposition with the optimum thickness. Through the study of the modifications in the dielectric and ac electrical properties of Au/PM-355 films. The variation in dielectric properties such as dielectric constant (ε'), dielectric loss factor (ε''), and ac conductivity (σ_{ac}) have been investigated in blank and the thin films.

3 Experimental details

In this study, the PM-355 samples were cleaned by ethanol and deposited by different Au thickness to form Au/PM-355 thin films. The optimum thickness was exposed to annealing and nitrogen, ion beams N_2^+, also compared with chloroform cleaning sample before deposition. These thin films and blank PM-355 were investigated by ac electrical properties.

A- Materials

PM-355 samples, allyl diglycol polycarbonate, with chemical composition $C_{12}H_{18}O_7$ is partly crystalline with dominant amorphous phase from Sigma-Aldrich, Germany. The samples size 1.5cm x 1cm with thickness 1mm, were cleaned by ethanol with purity 99.99% before deposition. The used chloroform contains 1 to 2% v/v ethanol as a preservative, AnalaR©, BDH Limited Poole England. The organic solvents were used with 0.3ml and spun at 1000rpm for 1min.

B- Thin films preparation and Au deposition

In this experiment, PM-355 samples were deposited by different Au thickness set to 300, 400, 500, 700, 1000, 1300, and 1500 nm using ion sputtering 1500 JFC device, see Fig. 1 High voltage

Fig. 1 — 1500 - JFC ion sputtering device.

power supply, 1KV DC/AC, was applied between 50mm diameter gold target and 70mm diameter specimen stage separated by 7cm distance.

C- Thin films treatment

i- Annealing

The optimum Au thickness thin film was annealing in air by using a thermostat oven at 140° C for 30 minutes. The rate of heating was 5° C per 1 min. and then the annealed sample was dropped out to cool to room temperature in air.

ii- Ion beam irradiation

Different thickness thin films, chloroform and annealed one are irradiated by N^+ ion beams that extracted from the copper conical anode and disc cathode ion source with radial extraction, see Fig. 2[50]. This ion source operating condition are the pressure, discharge current and discharge voltage equal to 3 x 10^{-4} mbar, 2 mA, 800 V respectively using 99.99 % nitrogen gas for 30 minutes. Finally, ac electrical conductivity measurements for these thin films were explained.

D- AC Electrical Properties

Electrical conductivity is an substantial device used to investigate the major factors as the crystal defects in structure and inner purity of semi-insulating crystalline solids. In this paper, the ac electrical properties of thin films were measured using EUCOL U2826 (LCR) meter over a frequency range 20 Hz - 5 MHz at room temperature. The electrical conductivity of a material depends on factors as the cross section area, conductor length, and temperature.

The analysis of ac conductivity and dielectric properties for thin films have been proceeded using impedance spectroscopy. This was done by applying a small ac signal towards the sample placing between two electrodes under spring pressure. Hence, a computer controlled impedance analyzer was used to measure the impedance parameters. While, the dielectric constant, έ, was calculated from the capacitance values that measured by computer from the following relation[51,52].

$$\varepsilon' = \frac{Cd}{\varepsilon_o A} \quad ...(1)$$

Anywhere ε_o is the permittivity of free space equal to 8.85 x 10^{-12} F.m^{-1}, C is the capacitance, d and A are the thickness and cross sectional area of sample respectively.

The dielectric material is having low electrical conductivity compared with metal and characterized by dielectric constant and dielectric loss. The dielectric analysis of conducting polymer gives us the information of its conductivity behavior. The temperature, frequency and compositions were used to measure the two essential electrical characteristics for dielectric properties of materials. The dielectric constant is the capacitive nature explains its capacity to store the electric charges and the dielectric loss is the conductive nature explicates its capacity to transfer the electronic charge[53].

4 Results and discussion

1- Thin Films without Nitrogen Ion Beam Irradiation

1.1- Deposition of different Au thickness on PM-355 thin films

Figures. 3-5 show the change of the dielectric constant, έ, dielectric loss, ε" and ac conductivity, σ_{ac}, as function of different logarithmic frequencies, log (f), at room temperature for different thickness Au(nm) deposited on PM-355 respectively. It is seen

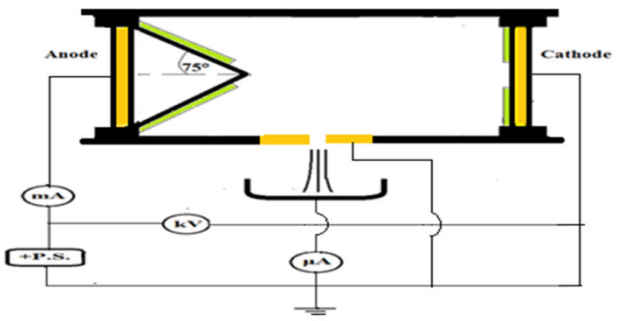

Fig. 2 — Copper conical anode and disc cathode ion source with radial extraction.

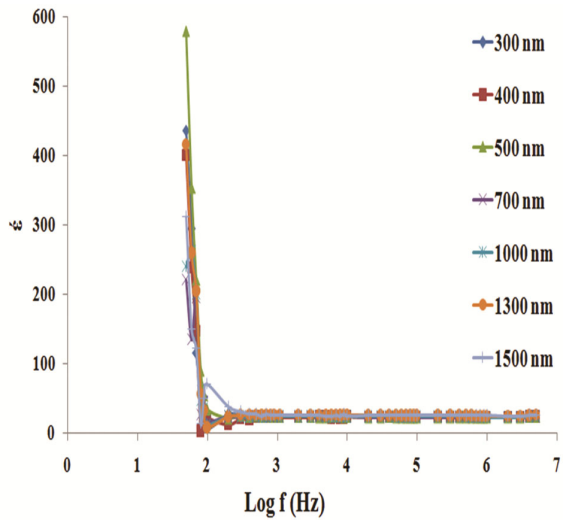

Fig. 3 — Dielectric constant versus log frequency range for different Au thickness deposited on PM-355.

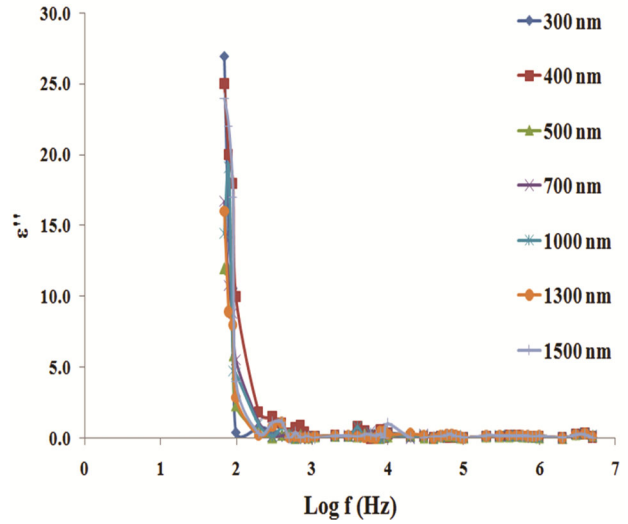

Fig. 4 — Dielectric loss versus log frequency range for different Au thickness deposited on PM-355.

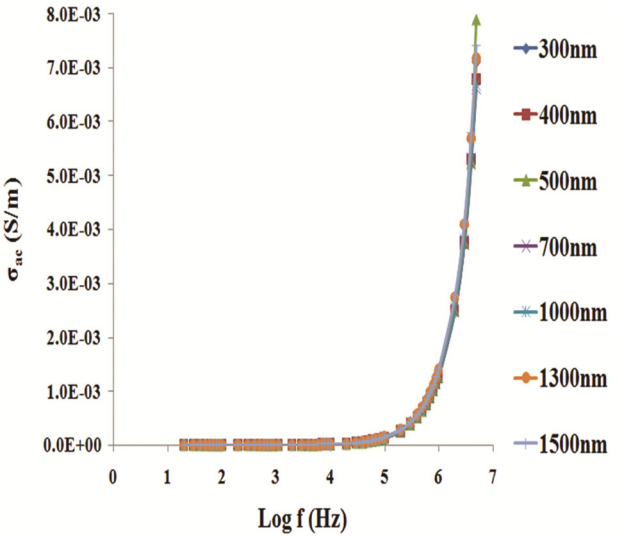

Fig. 5 — AC conductivity versus log frequency range for different Au thickness deposited on PM-355.

from Fig. 3 that the dielectric constant steeply decreases with an increase in log frequency and reaches a constant value from frequency, f, equal to 2 kHz (log f = 3.3 Hz) until 5 MHz (log f = 6.7 Hz). When f < 2 kHz, there is a sharp increase in έ value with decreasing frequency. Moreover, thin film with 500 nm Au thickness shows the highest dielectric constant compare to the remaining films that have lower ε'. It is the normal behavior of dielectrics that at low frequency the dipoles go ahead the field. Then, they begin to shift behind the field at high frequency and there is no excess ion diffusion in the direction of the field and that leading to decrease in dielectric constant[54].

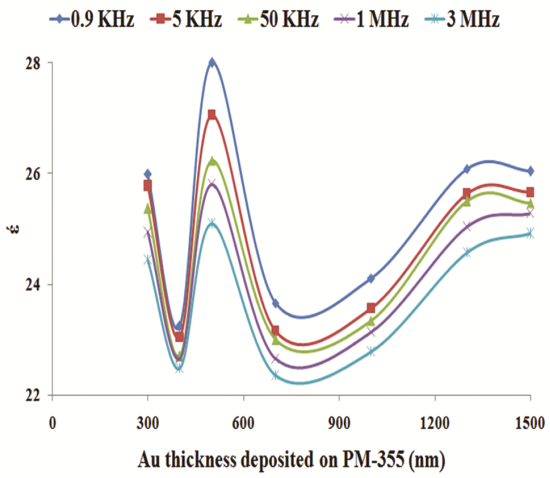

Fig. 6 — Dielectric constant versus different Au thickness at frequencies 0.9 kHz, 5 kHz, 50 kHz, 1 MHz and 3 MHz.

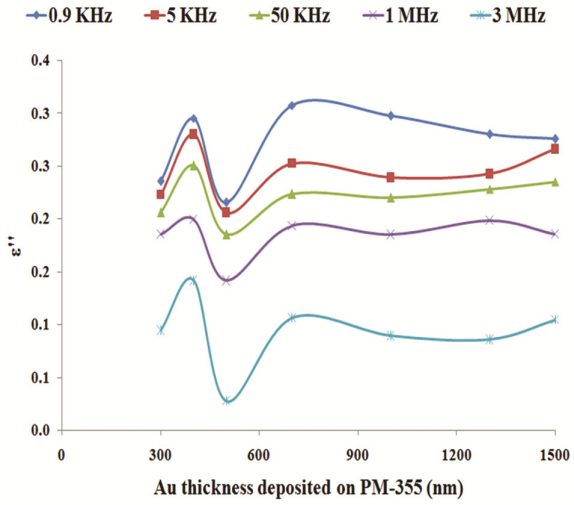

Fig. 7 — Dielectric loss versus different Au thickness at frequencies 0.9 kHz, 5 kHz, 50 kHz, 1 MHz and 3 MHz.

Dielectric loss shows the same behavior as dielectric constant. From Fig. 4, it is clear that the dielectric loss steeply decreases with an increase in log frequency and reaches a constant value from frequency, f, equal to 2 kHz (log f = 3.3 Hz) until 5 MHz (log f = 6.7 Hz). When f < 2 kHz, there is a sharp increase in ε" value with decreasing frequency. Moreover, thin film with 500 nm Au thickness shows the lowest dielectric loss compare to the remaining films that have higher ε". Hence from Fig. 5, it is observed that σ_{ac} varies linearly and increases steeply above the frequency 2 kHz (log f = 3.3 Hz) until 5 MHz (log f = 6.7 Hz). When f > 2 kHz, there is a sharp increase in σ_{ac} value with increasing frequency.

Figures. 6-8 show the variation of έ, ε", and σ_{ac} as function of different thickness nm Au deposited on

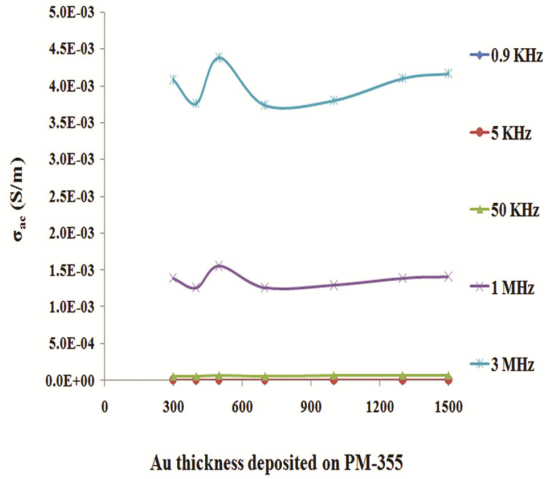

Fig. 8 — AC conductivity versus different Au thickness at frequencies 0.9 kHz, 5 kHz, 50 kHz, 1 MHz and 3 MHz.

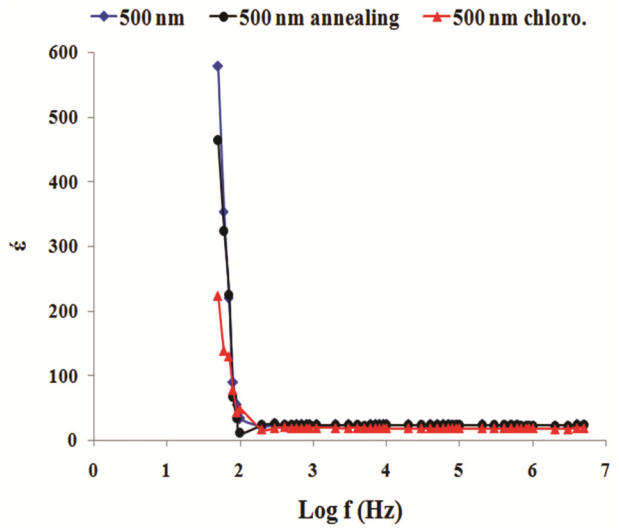

Fig. 9 — Dielectric constant versus log frequency range for 500 nm, 500 nm annealing and 500 nm chloroform.

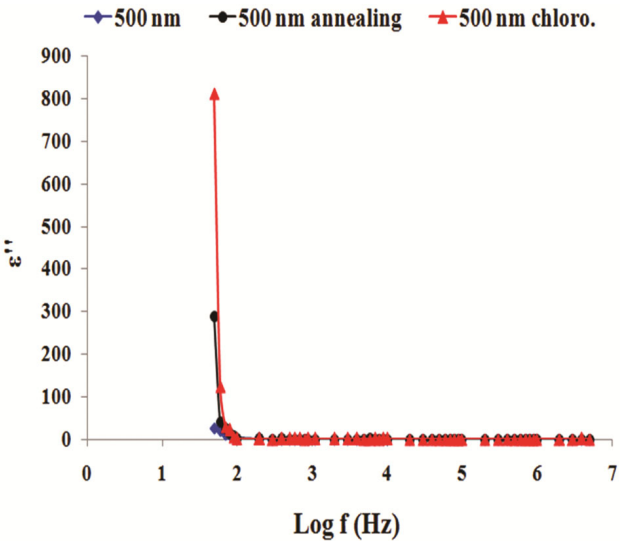

Fig. 10 — Dielectric loss versus log frequency range for 500 nm, 500 nm annealing and 500 nm chloroform.

PM-355 respectively at frequencies 0.9 kHz, 5 kHz, 50 kHz, 1 MHz, and 3 MHz. It is clear that from Fig. 6 that the highest έ value is at Au thickness equal to 500 nm for all frequencies and giving 28 at 0.9 kHz. For each frequency curve, at Au thickness < 500 nm then έ decreases by decreasing the thickness until reaching 400 nm thickness and increases again for 300 nm. Also, for Au thickness > 500 nm, έ decreases by increasing the thickness until reaching 700 nm and then increases to 1500 nm. Moreover, the highest έ is for the lower frequency value, 0.9 kHz, and 3 MHz has the lowest έ. Also, Fig. 7 shows that the optimum thin film, 500 nm Au has the lowest ε'' for all frequencies. Also, the highest ε'' is for the lower frequency value, 0.9 kHz, giving 0.2157 at 0.9 kHz and 3MHz has the lowest ε''. For each frequency curve, at Au thickness < 500 nm then ε'' increases by decreasing the thickness until reaching 400 nm thickness and decreases again for 300 nm. Hence, for Au thickness > 500 nm, ε'' increases by increasing the thickness until reaching 1500 nm.

Figure. 8 shows that the optimum thin film has the highest σ_{ac} for all frequencies. Also, the highest σ_{ac} is for the higher frequency value, 3 MHz, giving 4.38 x 10^{-3} S/m at 0.9 kHz and 0.9 kHz has the lowest σ_{ac}. For each frequency curve, at Au thickness < 500 nm, the σ_{ac} decreases by decreasing the thickness until reaching 400 nm thickness and then increases again for 300 nm. Hence, for Au thickness > 500 nm, σ_{ac} decreases by increasing the thickness until reaching 1500 nm.

1.2- Comparison between Optimum Thickness Au/PM-355 thin films with Annealing and Organic Solvents

In this part, the έ, ε'', and σ_{ac} comparisons were studied for the irradiated optimum thin film, the annealing one and the cleaned one by chloroform before deposition of 500 nm Au.

Figures. 9-11 show the variation in the έ, ε'' and σ_{ac} as function of different logarithmic frequencies, log (f), for 500 nm, 500 nm annealing, and 500 nm chloroform at room temperature, respectively. It is observed from Fig. 9 that the dielectric constant steeply decreases with an increase in log frequency and reaches a constant value from frequency, f, equal to 9 kHz (log f = 3.95 Hz) until 5 MHz (log f = 6.7 Hz). When f < 9 kHz, there is an increase in έ value with decreasing frequency. Moreover, thin film with 500 nm Au shows the highest έ, 24.16, followed

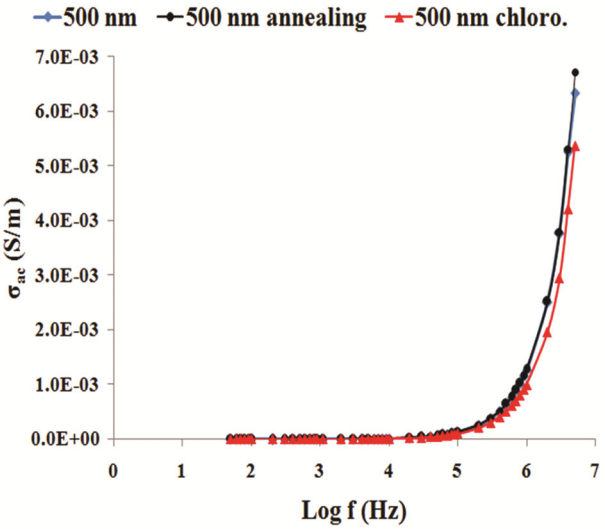

Fig. 11 — AC conductivity versus log frequency range for 500 nm, 500 nm annealing and 500 nm chloroform.

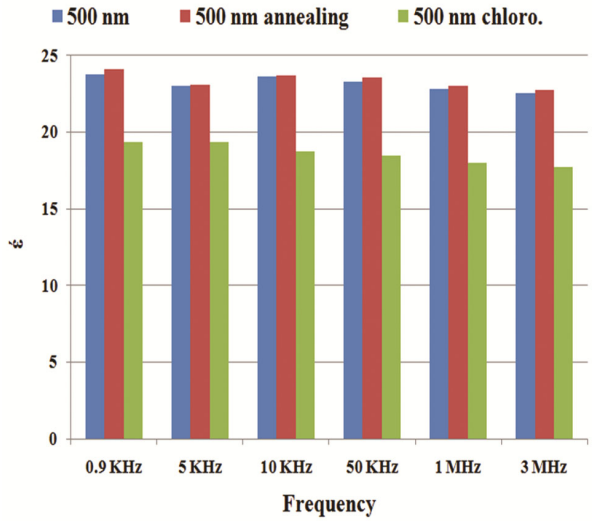

Fig. 12 — Dielectric constant versus frequencies (0.9, 5, 10, 50) kHz, (1, 3) MHz for 500 nm, 500 nm annealing and 500 nm chloroform.

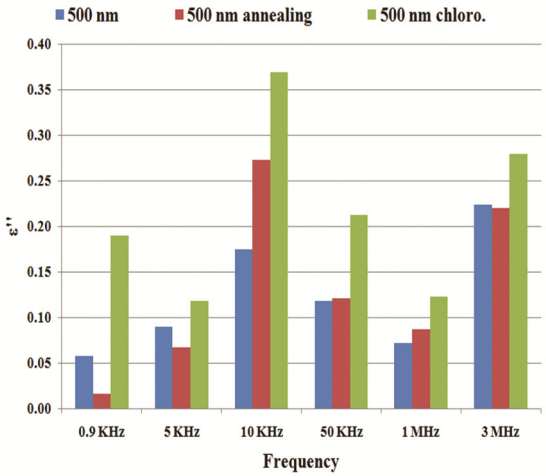

Fig. 13 — Dielectric loss versus frequencies (0.9, 5, 10, 50) KHz, (1, 3) MHz for 500 nm, 500 nm annealing and 500 nm chloroform.

by the annealing one that is in the middle giving 23.84. In opposite, thin film with 500 nm Au cleaned before by chloroform that has lower ε' of 19.29. It is shown from Fig. 10 that the dielectric loss steeply decreases with an increase in log frequency and reaches a constant value from frequency, f, equal to 9 kHz (log f = 3.95 Hz) until 5 MHz (log f = 6.7 Hz). When f < 9 kHz, there is an increase in ε" value with decreasing frequency. Moreover, thin film with 500 nm Au cleaned before by chloroform that has higher ε" giving 0.194. In opposite, thin film with 500 nm Au, has 0.12, shows the ε" and then the annealing one, 0.169, is in the middle between the other two thin film.

It is deduced from Fig. 11 that the ac conductivity is nearly constant with an increase in log frequency and increases from frequency, f, equal to 9 kHz (log f = 3.95 Hz) reaching maximum at 5 MHz (log f = 6.7 Hz). Moreover, 500 nm Au thin film treated with annealing has the highest σ_{ac}, 6.72 x 10^{-3} S/m and followed by 500 nm Au thin film with 6.33 x 10^{-3} S/m. Hence, thin film with 500 nm Au cleaned before by chloroform that has lowest σ_{ac} equal to 5.37 x 10^{-3} S/m.

Figures. 12,13 show the variation in the έ and ε" as function of different frequencies equal to (0.9, 5, 10, 50) kHz, (1, 3) MHz for 500 nm, 500 nm annealing, and 500 nm chloroform at room temperature, respectively. It is clear from Fig. 12 that the έ is lowest for 500 nm chloroform, but thin film of 500 nm and annealing one have nearly close to each other with higher έ. At 0.9 KHz, a 500 nm annealing thin film is slowly high έ of 24.13 than without annealing that equal to 23.77 and compared with the έ chloroform thin film equal to 19.37. For each thin film type, έ value decreases from frequency equal to 0.9 kHz until 3 MHz. From Fig. 13, ε" is lowest for 500 nm annealing thin film compared with 500 nm chloroform has the highest ε". At 0.9 kHz, a 500 nm annealing thin film has ε" equal to 0.0156 than without annealing that equal to 0.0576 and compared with the ε" chloroform thin film equal to 0.19.

Figure. 14(a,b) shows the change in σ_{ac} with different frequencies equal to (0.9, 5, 10, 30, 50) kHz, (1, 2, 3, 4, 5) MHz for 500 nm, 500 nm annealing, and 500 nm chloroform at room temperature, respectively.

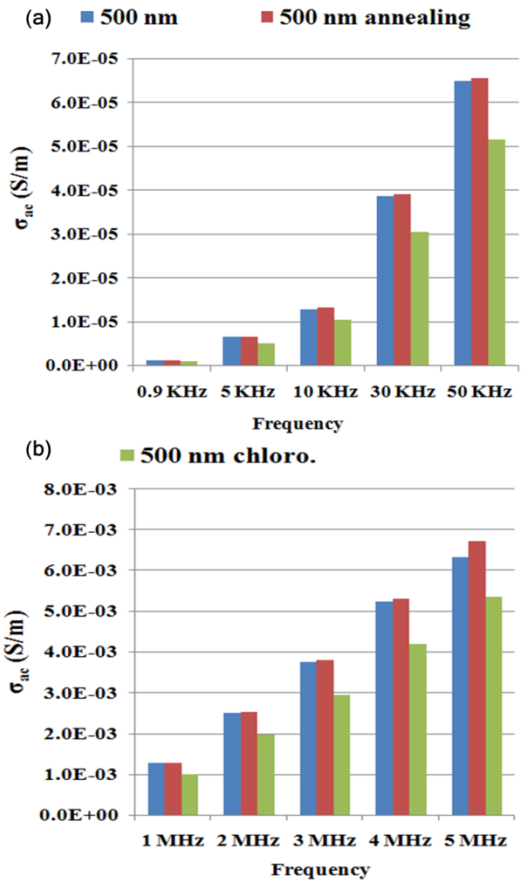

Fig. 14 — AC conductivity versus frequencies: a- (0.9, 5, 10, 30, 50) kHz, b- (1, 2, 3, 4, 5) MHz for 500 nm, 500 nm annealing and 500 nm chloroform.

It is clear from Fig. 14(a) that σ_{ac} is lowest for 500 nm chloroform, but thin film of 500 nm and annealing one have nearly close to each other with higher σ_{ac} . At 0.9 kHz, a 500 nm annealing thin film is high σ_{ac} of 1.2 x 10^{-6} S/m than without annealing that equal to 1.7 x 10^{-6} S/m and compared with σ_{ac} of chloroform thin film that equal to 9.71 x 10^{-7} S/m. For each thin film type, σ_{ac} value increases from frequency equal to 0.9 kHz until 3 MHz. Fig. 14(b) shows that σ_{ac} is also lowest for 500 nm chloroform, but thin film of 500 nm and annealing one have nearly close to each other with higher σ_{ac} . At 5 MHz, a 500 nm annealing thin film is high σ_{ac} of 6.72 x 10^{-3} S/m than without annealing that equal to 6.33 x 10^{-3} S/m and compared with σ_{ac} of chloroform thin film that equal to 5.37 x 10^{-3} S/m. For each thin film type, σ_{ac} value increases from frequency equal to 1 MHz until 5 MHz.

2- Comparison of Thin Films without and with Nitrogen Ion Beam Irradiation

In this part, for έ, ε", and σ_{ac} comparisons were studied for the 500 nm, annealing and chloroform thin films and with N_2^+ ion beams thin films. Fig. 15,16 show the comparison of έ and σ_{ac} as function of different logarithmic frequencies, log (f), for 500 nm and 500 nm irradiated by ion beam thin films at room temperature, respectively. From Fig. 15, it is clear that the 500 nm thin film without ion beam gives maximum έ than irradiated one. The έ starts from 578.72 and 356.23 for 500 nm and irradiated ion beam 500 nm thin films respectively. Also, έ curves are steeply decreases with an increase in log frequency and reaches a constant value from frequency, f, equal to 0.6 kHz (log f = 2.78 Hz) until 5 MHz (log f = 6.7 Hz). From Fig. 16, the 500 nm thin film without ion beam gives maximum σ_{ac} than

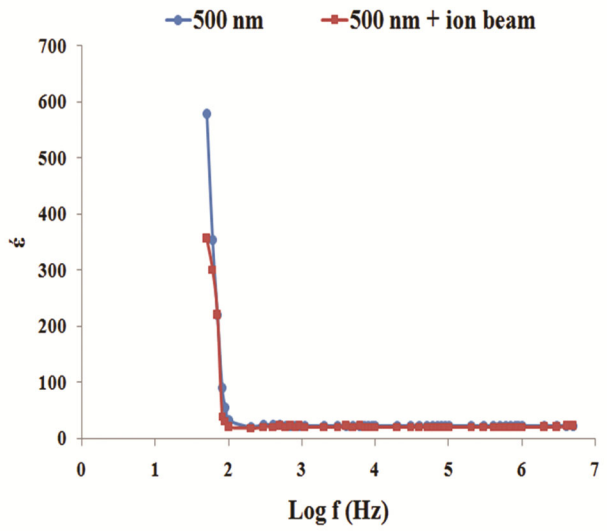

Fig. 15 — Dielectric constant versus log frequency range for 500 nm and with ion beam thin films.

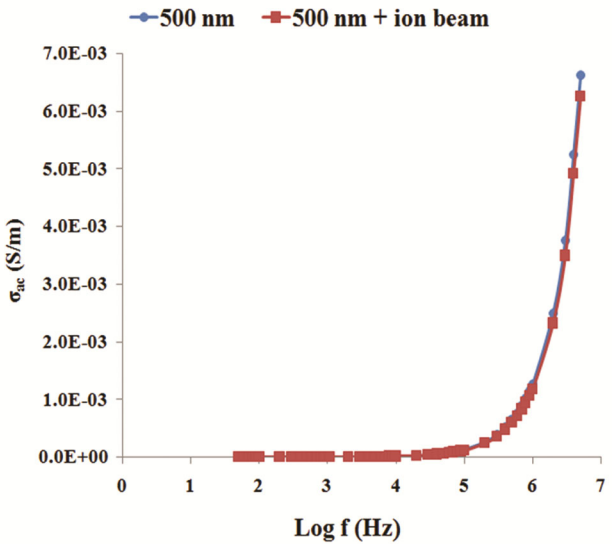

Fig. 16 — AC conductivity versus log frequency range for 500 nm and with ion beam thin films.

irradiated one. The σ_{ac} reaching to 6.63 x 10^{-3} S/m for 500 nm thin film and decreased to 6.25 x 10^{-3} S/m for irradiated ion beam 500 nm thin film at frequency 5 MHz. Also, σ_{ac} curves varies linearly at low frequencies and increases steeply above the frequency 0.6 kHz (log f = 2.78 Hz) until 5 MHz (log f = 6.7 Hz).

Figures. 17,18 show the comparison of έ and σ_{ac} as function of different logarithmic frequencies, log (f), for 500 nm annealing thin film and irradiated one by ion beam at room temperature, respectively. From Fig. 17, it is clear that the 500 nm annealing thin film gives maximum έ than irradiated one with ion beam. The έ starts from 623.77 and 464.23 for 500 nm annealing and irradiated ion beam thin films respectively. Also, έ curves are steeply decreases with an increase in log frequency and reaches a constant value from frequency, f, equal to 0.6 kHz (log f = 2.78 Hz) until 5 MHz (log f = 6.7 Hz). From Fig. 18, the 500 nm annealing thin film gives maximum σ_{ac} than ion beam irradiated one. The σ_{ac} reaching to 6.72 x 10^{-3} S/m and 4.91 x 10^{-3} S/m for 500 nm annealing thin film and irradiated ion beam one at frequency 5 MHz, respectively. Also, σ_{ac} curves varies linearly at low frequencies and increases steeply above the frequency 0.6 KHz (log f = 2.78 Hz) until 5 MHz (log f = 6.7 Hz).

Figures. 19,20 show the comparison of έ and σ_{ac} as function of different logarithmic frequencies, log (f),

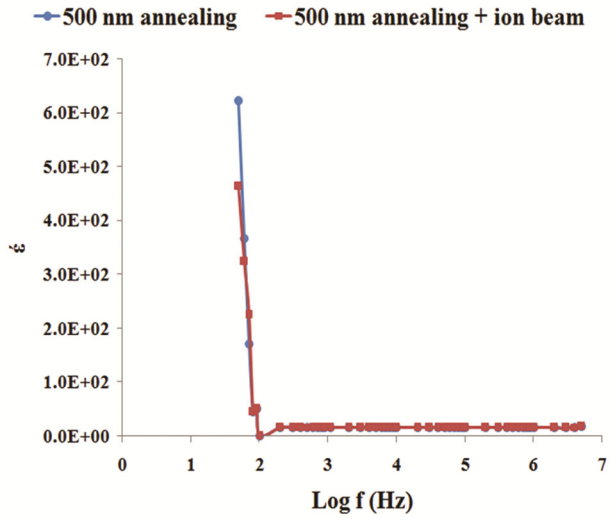

Fig. 17 — Dielectric constant versus log frequency range for 500 nm annealing and with ion beam thin films.

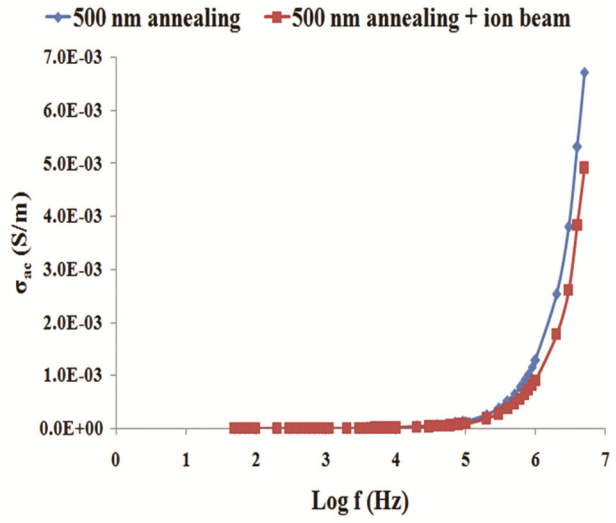

Fig. 18 — AC conductivity versus log frequency range for 500 nm annealing with ion beam thin films.

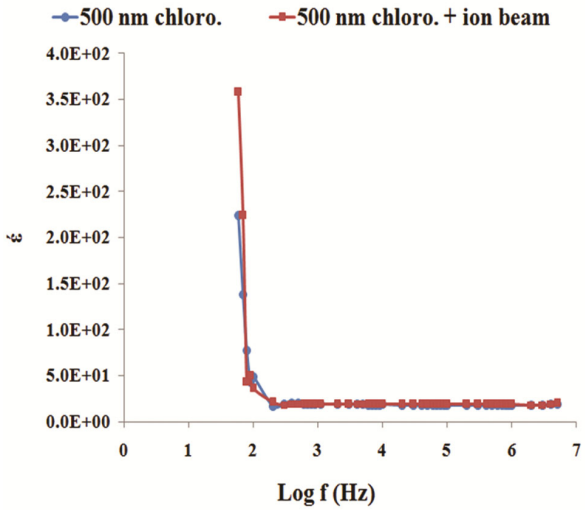

Fig. 19 — Dielectric constant versus log frequency range for 500 nm chloroform and with ion beam thin films.

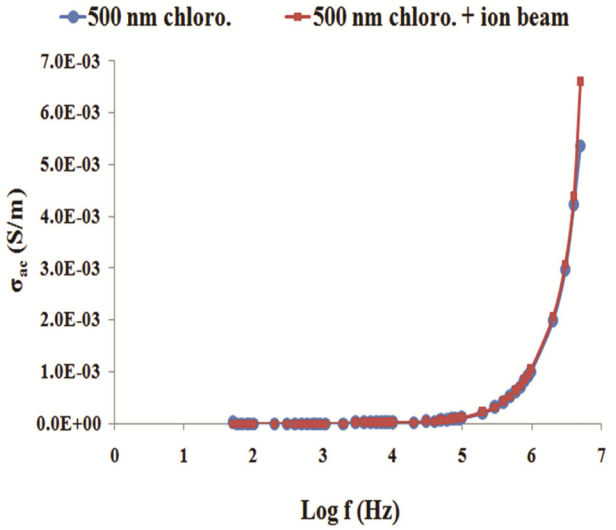

Fig. 20 — AC conductivity versus log frequency range for 500 nm chloroform with ion beam thin films.

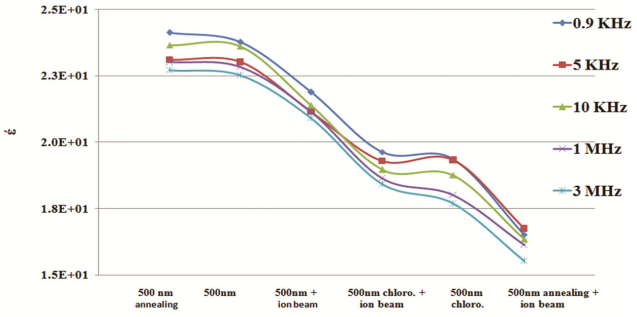

Fig. 21 — Dielectric constant versus 500 nm, 500 nm annealing, 500 nm chloroform and their irradiated with ion beam thin films at 0.9kHz, 5kHZ, 10kHz, 1MHz and 5MHz.

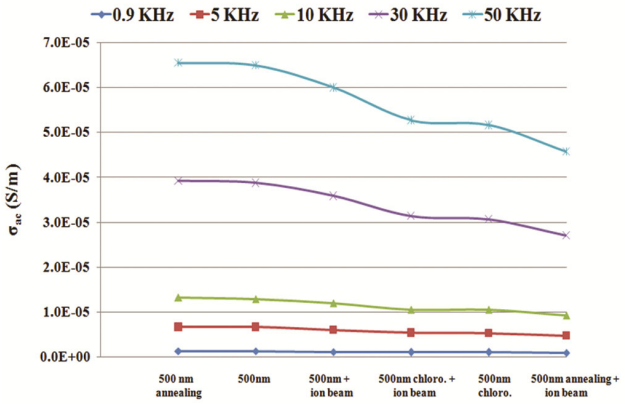

Fig. 22 — AC conductivity versus 500 nm, 500 nm annealing, 500 nm chloroform and their irradiated with ion beam thin films at 0.9, 5, 10, 30 and 50 kHz.

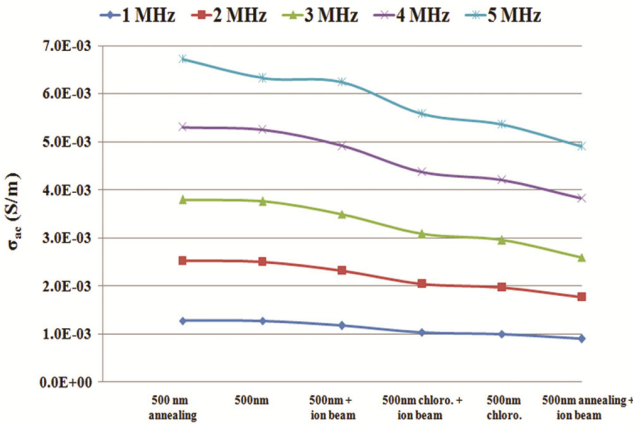

Fig. 23 — AC conductivity versus 500 nm, 500 nm annealing, 500 nm chloroform and their irradiated with ion beam thin films at 1, 2, 3, 4 and 5 MHz.

for 500 nm chloroform thin film and irradiated one by ion beam thin films respectively at room temperature. From Fig. 19, it is clear that the 500 nm chloroform thin film irradiated with ion beam gives maximum έ than that without ion beam. The έ starts from 129.04 and 223.04 for 500 nm chloroform and irradiated ion beam thin films respectively. Also, έ curves are steeply decreases with an increase in log frequency and reaches a constant value from frequency, f, equal to 0.6 kHz (log f = 2.78 Hz) until 5 MHz (log f = 6.7 Hz). From Fig. 20, the 500 nm chloroform irradiated with ion beam thin film gives maximum σ_{ac} than that without ion beam. The σ_{ac} reaching to 5.37 x 10^{-3} S/m and 6.59 x 10^{-3} S/m for 500 nm chloroform thin film and irradiated ion beam one at frequency 5 MHz respectively. Also, σ_{ac} curves varies linearly at low frequencies and increases steeply above the frequency 0.6 kHz (log f = 2.78 Hz) until 5 MHz (log f = 6.7 Hz).

Finally, the variation in έ and σ_{ac} versus 500 nm, 500 nm annealing, 500 nm chloroform, and their ion beam irradiation at different frequencies have been compared. Fig. 21 shows the variation in dielectric constant versus 500 nm, 500 nm annealing, 500 nm chloroform, and their ion beam irradiation at frequencies equal to (0.9, 5, 10) kHz, and (1, 3) MHz. It is clear that the highest έ is for 500 nm thin film after annealing followed by 500 nm thin film and the lowest έ is for 500 nm annealing thin film after irradiation with ion beam.

Figures. 22,23 show the variation in ac conductivity versus 500 nm, 500 nm annealing, 500 nm chloroform, and their ion beam irradiation at frequencies equal to (0.9, 5, 10, 30, 50) kHz, and (1, 2, 3, 4, 5) MHz respectively. It is clear from Fig. 22 that the highest σ_{ac} is for 500 nm thin film after annealing and very close to 500 nm thin film and then followed by 500 nm thin film irradiated by ion beam. However, the lowest σ_{ac} is for 500 nm annealing thin film after irradiation with ion beam. Moreover, the Fig. 23 indicates that the highest σ_{ac} is for 500 nm thin film after annealing followed by 500 nm thin film. Then, the lowest σ_{ac} is for 500 nm annealing thin film after irradiation with ion beam.

5 Conclusion

Determination of the optimum thickness of Au deposited on PM-355 to form thin film with good ac electrical conductivity and dielectric properties were studied. Then, the organic solvents cleaning before Au deposition plays an important role in the enhancement of thin film properties. Before ion beam irradiation, the highest έ is for ethanol cleaning PM-355 samples before Au deposition with optimum thickness and also that after annealing. Dielectric

constant and ac conductivity values for ethanol optimum Au thickness and that after annealing thin films at the frequency range 20 Hz – 5 MHz. The chloroform cleaning thin film gives the lowest έ and σ_{ac} values compared with the highest dielectric loss value. The decreased in dielectric constant with increasing logarithmic frequency reaching constant at higher frequencies refers to the attributed of dipoles to orient themselves in the direction of applied field. Hence, thin film conductivity depends on its dielectric nature.

The effect of annealing on optimum thickness increases both έ and σ_{ac} by nearly 6.7 %. Also, the irradiation of nitrogen ion beam that extracted from the conical anode and disc cathode ion source effects on thin films ac electrical and dielectric properties. The ion irradiation thin film gives the change in έ and σ_{ac} values that decreased by (7.153, 5.73 %) for ethanol optimum thickness and (26.95, 6.3 %) after annealing thin film than of its value before ion irradiation respectively. In the opposite case, έ and σ_{ac} values for chloroform deposition thin film that increased by 72.84 % and 22.72 % of its value before irradiation respectively.

Moreover, among the comparison for all thin films without and with ion irradiation. It is concluded that the highest έ for optimum Au thickness after annealing thin film and gives the lowest value after the ion beam irradiation. In other meaning, the ion irradiation decreases ac electrical and dielectric properties for thin films and annealing processes except for the chloroform cleaning before Au deposition that increases. Finally, it is necessary to form membrane/catalyst in fuel cells used thin film with ethanol cleaned then treated by annealing and nitrogen ion beam that gives the minimum value of conductivity.

References

1 Ren X, Li H, Fu Q, Chu Y & Li K, *Surf Coat Technol*, 232 (2013) 821.
2 Zhang Y, Hu Z, Li H & Ren J, *Ceram Int*, 40 (2014) 14749.
3 Gauter S, Haase F & Kersten H, *Thin Solid Films*, 669 (2019) 8.
4 Belosludtsev A, Houška J, Vlček J, Haviar S, Čerstvý R, Rezek J & Kettner M, *Ceram Int*, 43 (2017) 5661.
5 Bahramian A, Eyraud M, Vacandio F & Knauth P, *Surf Coating Technol*, 345 (2018) 40.
6 Sun Y, Flis-Kabulska I & Flis J, *Mater Chem Phys*, 145 (2014) 476.
7 Tang C C, Stueber M, Seifert H J & Steinbrueck M, *Corrosion Rev*, 35 (2017) 141.
8 Anders A, *Thin Solid Films*, 518 (2010) 4087.
9 Gu C, Sui Z, Li Y, Chu H, Ding S, Zhao Y & Jiang C, *Appl Surf Sci*, 433 (2018) 306.
10 Li X, Bai Q, Yang J, Li Y, Wang L, Wang H, Ren S, Liu S & Huang W, *Vacuum*, 89 (2013) 78.
11 Dai W, Ke P, Moon M W, Lee K R & Wang A, *Thin Solid Films*, 520 (2012) 6057.
12 Dai W, Ke P & Wang A, *Vacuum*, 85 (2011) 792.
13 Belosludtsev A, Houška J, Vlček J, Haviar S, Čerstvý R, Rezek J & Kettner M, *Ceram Int*, 43 (2017) 5661.
14 Bahramian A, Eyraud M, Vacandio F & Knauth P, *Surf Coating Technol*, 345 (2018) 40.
15 Sun Y, Flis-Kabulska I & Flis J, *Mater Chem Phys*, 145 (2014) 476.
16 Nesher G, Marom G & Avnir D, *Chem Mater*, 20 (2008) 4425.
17 Ghanipour M & Dorranian D, *J Nanomater* 2013 (2013) 1.
18 Sakthivel P, Murugan R, Asaithambi S, Karuppaiah M, Rajendran S, Ravi G, *J Chem Solids*, 126 (2019) 1.
19 Shahpanah M, Mehrabian S, Firouzjah M A & Shokri B, *Surf Coat Technol*, 358 (2019). 91.
20 Lal S, Grady N K, Kundu J, Levin C S, Lassiter J B & Halas N J, *Chem Soc Rev*, 37 (2008) 898.
21 Yue G, Su S, Li N, Shuai M, Lai X, Astruc D & Zhao P, *Coord Chem Rev*, 311 (2016). 75.
22 Kim G H, Rathi S, Baik J M & Yi K S, *Curr Appl Phys*, 15 (2015) 1107.
23 Choi J, Cho J, Roh C W, Kim B S, Choi M S, Jeong H, Ham H C & Lee H, *Appl Catal B: Environ*, 247 (2019) 142.
24 Moazzez B, O'Brien S M & Merschrod E F, *Sensors*, 13 (2013) 7021.
25 Tassin P, Koschny T, Kafesaki M & Soukoulis C M, *Nature Photon*, 6 (2012) 259.
26 Nordström M, Johansson A, Sánchez Nogueron E, Calleja M & Boisen A, *Microelectron Eng*, 78 (2005) 152.
27 Hugall J T, Finnemore A S, Baumberg J J, Steiner U & Mahajan S, *Langmuir*, 28 (2012) 1347.
28 Fink D, Fundamentals of Ion-Irradiated Polymers (Springer-Verlag, Berlin, 2004).
29 Wise D L, Wnek G E, Trantolu D J, Cooper T M & Gresser J D, Electrical and Optical Polymer Systems: Fundamentals, Methods & Applications (Marcel Dekker, Inc, New York, 1998).
30 Schnell H, Chemistry and Physics of Aromatic Polycarbonate (Interscience Publishers, New York, 1964).
31 Alegaonkar P S, Bhoraskar V N, Balaya P & Goyal P S, *Appl Phys Lett*, 80 (2002) 640.
32 Kam W, Ong Y S, Lim W H & Zakaria R, *Opt Laser Eng* 55 (2014) 1.
33 Naik D G & Nadkarni V S, *Radiat Phys Chem*, 156 (2019) 259.
34 Fromm M, Kodaira S, Kusumoto T, Barillon R & Yamauchi T, *Polym Degrad Stab*, 161 (2019) 213.
35 Patel A K & Acharya N K, *Int J Hydrog Energy*, 43 (2018) 21675.
36 Lee Y H, Park T, Chang I, Ji S & Cha S W, *Int J Hydrog Energy*, 37 (2012) 18471.
37 Nafarizal N, *Proc Chem*, 20 (2016) 93.
38 Sidelev D V, Bleykher G A, Grudinin V A, Krivobokov V P, Bestetti M, Syrtanov M S, Erofeev E V, *Surf Coat Technol*, 334 (2018) 61.
39 Chen B, Chen G, Wanga W, Cai H, Yao L, Chen S & Huang Z, *J Sol Energy*, 176 (2018) 98.

40 Bonu V, Jeevitha M, Kumar V P & Barshilia H C, *Surf Coat Technol*, 357 (2019) 204.
41 Swann S, *Phys Techno1*, 19 (1988) 67.
42 Constantin D G, Apreutesei M, Arvinte R, Marin A, Andrei O C & Munteanu D, 7th *Int Conf Mater Sci Eng – BRAMAT*, Braşov, (2011) 29.
43 Caillard A, El'Mokh M, Lecas T & Thomann A L, *Vacuum*, 147 (2018) 82.
44 Bernareggi M, Chiarello G L, West G, Ratova M, Ferretti A M, Kelly P & Selli E, *Catal Today J*, 326 (2019) 15.
45 Shapovalov V I, Useinov A S, Kravchuk K S, Gladkikh E V, Kozin A A & Smirnov V V, *Glass Phys Chem*, 43 (2017) 477.
46 Kaziev A V, Tumarkin A V, Leonova K A, Kolodko D V, Kharkov M M & Ageychenkov D G, *Vacuum*, 156 (2018) 48.
47 Chen X, Wang J S, Li H Y, Huang K L & Sun G S, *Res Chem Interm* 37 (2011) 441.
48 Einollahzadeh-Samadi M & Dariani R S, *Appl Surf Sci*, 280 (2013) 263.
49 Mahmoud G, Kiomars Y, Abbas A, Hamidreza P, Alireza H & Homa H, *J Plasma Fusion Res Ser*, 7 (2006) 307.
50 Radwan S I, Abdel Samad S & El-Khabeary H, *J Nucl Ene Sci Power Generat Technol*, 10 (2021) 3.
51 Mujahid M, Singh P, Srivastava D S, Gupta S, Avasthi D K & Kanjilal D, *Radiat Meas*, 38 (2004) 197.
52 Rathore B S, Gaur M S & Singh K S, *J Ther Anal Calorim*, 111 (2013) 647.
53 Shanthala V S, Devi S N S & Murugendrappa M V, *J Appl Phys*, 8 (2016) 83.
54 Patil B S, Prakash N, J, Kumar R, Tripathi S K & Thakur N, *J Nano Electron Phys*, 5 02019 (2013) 4.